Performance and Aging of Graphene Oxide/Polyurethane Nanocomposites

D. G. Goodwin Jr.[*], C. Bernard[*], V. Reipa[**], D. Jacobs*, T. Nguyen*, and L. Sung[*]

[*]Materials and Stuctural Systems Division, Engineering Laboratory
[**]Biosystems and Biomaterials Division, Materials Measurement Laboratory
National Institute of Standards and Technology, Gaithersburg, MD, USA

ABSTRACT

There is potential to use graphene oxide (GO) nanofillers to enhance the mechanical strength, thermal properties, and barrier properties of polymers used in coatings applications. Although the properties of graphene are generally superior to GO, GO nanofillers are more cost effective and oftentimes easier to incorporate into polymer matrices. In order to assesss the benefits and limitations of GO use as a nanofiller in polymer coatings, this study measured the performance properties of GO/waterborne polyurethane (WBPU) nanocomposites relative to those of unfilled WBPU. The potential for GO release was also studied to determine coating durability and assess the environmental health and safety (EHS) risks of GO/WBPU nanocomposites with respect to aging under accelerated ultraviolet (UV)-weathering conditions.

Keywords: graphene oxide, polyurethane, polymer nanocomposites, weathering, nanomaterial release, performance properties

1 INTRODUCTION

Commercial products often utilize nanoparticle fillers embedded in polymers to improve performance properties.[1-2] In particular, graphene nanomaterials, which consist of a single layer sheet of sp^2-hybridized carbon, have high electrical conductivity, mechanical strength, thermal stability, and barrier properties which can be transferred to a polymer matrix for performance improvement.[3] However, other graphene-family nanomaterials (GFNs), such as GO and reduced graphene oxide (rGO) are cheaper and easier to process since they can be well-dispersed as individual flakes using the oxygen functional groups present at the edges and other defect sites within the graphitic structure. Although GO may improve the processing efficiency and cost of GFN nanocomposite production, the property improvements imparted by GO may be less than those imparted by graphene due to the disrupted sp^2 network in the GO structure.[3] For that reason, this study examines the performance properties of GO embedded in a polymer matrix relative to an unfilled polymer control. WBPU was chosen as the polymer type since it is widely used in coatings applications. The performance properties studied, which were relevant to coatings applications, included mechanical strength, thermal conductivity, flammability, and corrosion-related properties such as water sorption, oxygen permeability, and electrochemical corrosion resistance.

The service life and EHS risks are also important factors to consider in the development of this new type of coating. During the many stages of a coating's life-cycle, the polymer matrix is susceptible to mechanical wear, photolysis, weathering, and thermal, biological, and chemical degradation.[4] For polymer nanocomposites (PNCs), these processes can increase the potential for GO exposure and release as the polymer matrix degrades. When carbonaceous nanomaterials (CNMs), such as GO, release from polymers, the main challenge is differentiating the CNMs and polymer from each other since they both contain carbon and oxygen.[5] To date, most CNM release studies from PNCs have largely focused on mechanical abrasion and UV-weathering with carbon nanotube/PNCs.[6]

In this study, UV-Visible (UV-Vis) and Raman spectroscopy methods were used to measure GO release. The interference of polymer fragments released simultaneously with GO was assessed to determine method limitations. The release scenario was simulated by the NIST SPHERE (Simulated Photodegradation via High Energy Radiant Exposure) under controlled temperature and humidity conditions; the SPHERE has been used previously to accelerate testing of PNC degradation and nanomaterial release by UV-irradiation.[7] Collectively, the service life with respect to GO release and the performance properties of GO/WBPU nanocomposites were considered to help evaluate the viability of GO/PNC use in coatings applications.

2 EXPERIMENTAL[◊]

2.1 Nanocomposite Preparation

The WBPU used in this study was a one-component, anionic dispersion of an aliphatic polyester urethane resin in water (50 % mass fraction) and n-methyl-2-pyrrolidone (NMP) (15 % mass fraction) (Bayhydrol 110, Bayer MaterialScience LLC). GO was prepared by the University of Texas, Austin, TX, using the Hummers method.[8] The GO had a thickness of approximately 0.8 nm to 1.0 nm and lateral dimensions between a few hundred nanometers to a few micrometers (measured by atomic force microscopy

[◊] *Certain commercial product or equipment is described in this paper in order to specify adequately the experimental procedure. In no case does such identification imply recommendation or endorsement by the National Institute of Standards and Technology, nor does it imply that it is necessarily the best available for the purpose.*

(AFM)), similar to the results reported previously. Both unfilled WBPU and GO/WBPU nanocomposites were prepared as described elsewhere.[9] For method development of GO release measurements, another commercial type of GO (ACS Materials, thickness of 0.6 nm to 1.2 nm, and lateral dimensions of 0.5 µm to 2 µm measured with AFM by the manufacturer) was used because of its availability and ease of dispersion at high mass concentrations.

2.2 Performance Properties

Mechanical properties were characterized using a dynamic mechanical thermal analyzer (DMTA) in transient mode at a 0.5 mm/s extension rate on dog bone specimens having a 20 mm gage length and a 3.30 mm width. Oxygen permeability was measured on 20 mm x 50 mm film samples using a custom-modified Oxtran-100 coulometric permeation apparatus. The analysis of O_2 relied on the reaction between O_2 and H_2 utilizing a catalysis-based sensor.[10] Flammability properties were evaluated using a microcombustion micrometer under N_2, as described elsewhere.[11] Thermal conductivity was measured using a hot disk Thermal Constants Analyzer.[12] This measurement was made at 24 ºC with a power of 0.02 W applied for 20 s, using 10 replicate specimens having a diameter of 50 mm and a thickness of (5-7) mm.

Water vapor uptake as a function of relative humidity (RH), was obtained using an IGAsorp Moisture Sorption Analyser having a mass resolution of 0.1 µg with a RH accuracy of ± 1 % from 0 % to 90 % RH. For each RH, a PNC specimen of approximately 8.5 mg was first loaded into a holder and dried in the analyser until a minimum mass was reached. The sorption experiment was then started until the amount of water uptake in the specimen at that particular RH reached an equilibrium, usually between 500 min and 1000 min, depending on the RH levels. All sorption experiments from 0 % RH to 90 % RH were conducted at 25 ºC, and the results from three specimens were averaged. Corrosion measurements were made on specimens (ten replicate thickness measurements made per specimen with scanning electron microscopy (SEM)) coated onto steel in the presence of NaCl (3.5 % mass fraction). The voltage/current profiles of the coatings were measured at different time points up to 240 h. For brevity, the uncertainty listed out in Section 3 is the standard deviation associated with measurements on either ten replicates unless otherwise indicated in this section.

2.3 UV-Weathering

Specimens were mounted in a specially designed sample holder using a front cover made of quartz to contain released materials and allow UV light to reach the specimens. Specimens were aged at 140 W/m^2 (at wavelengths from 295 nm to 400 nm), 55 °C, and 0 % RH.

2.4 Run-off Suspension Collection

After UV-weathering, each specimen was separately sprayed in its sample holder cell with ultrapure water (0.18 MΩ·m) for 5 min, and approximately 5 mL of run-off suspension was collected from the cell drain. Spraying was accomplished using a chromatographic atomizer attached to an Erlenmeyer flask (see Figure 1). Details can be found in a previous publication.[13]

2.5 UV-Vis Spectroscopy

An aqueous GO stock suspension (ACS Materials) at 10 mg/mL was serially diluted for UV-Vis spectroscopy measurements (Agilent 8453 UV-Vis spectroscopy system). For GO + WBPU suspensions, GO suspensions at varied mass concentration were separately prepared with each containing the same WBPU concentration. The run-off suspension was analzyed in the same way.

2.6 Raman Spectroscopy

GO suspensions (Section 2.4) and run-off suspensions were analyzed with a Kaiser Holospec F1.8 Raman spectrometer, equipped with a thermoelectrically cooled CCD detector (Apogee, Inc.) using a 488 nm Argon laser (Lexel, Inc.); the spectrometer was calibrated using laser plasma line frequencies. Suspension aliquots of 0.5 mL were measured in a rectangular plastic cuvette (NSG, Inc.). Spectra were accumulated for 50 s with 180 mW laser power. A linear background correction was applied from 1200 cm^{-1} to 1500 cm^{-1}.

3 RESULTS AND DISCUSSION

At the highest GO/WBPU loading studied, 2 % mass fraction, the incorporation of GO nanofillers was shown to improve the performance properties of WBPU. The GO increased the modulus and yield strength of WBPU by approximately 300 % (from (200 ± 25) MPa to (600 ± 90) MPa) and 200 % (from (13 ± 1) MPa to (26 ± 3) MPa), respectively. The thermal conductivity increased from (0.23 ± 0.02) W/m·K for unfilled WBPU to (0.33 ± 0.03) W/m·K for the GO/WBPU nanocomposite. The burning heat release rate (HRR), which is often associated with flammability, decreased by approximately 43 % (from (240 ± 15) W/g to (137 ± 8) W/g with GO incorporation. It has been shown previously that a reduced HRR depends, in large part, on the ability of nanofillers to form a protective layer that insulates unburnt polymer from thermal energy incident on the material surface. Thus, the decreased HRR provides one type of measurement that indicates flammability reduction of WBPU by GO incorporation.

The oxygen permeability, water sorption, and corrosion resistance were also measured for GO/WBPU nanocomposites since GFNs have been shown to have excellent barrier properties. These barrier properties are of strong interest in coatings applications since they can potentially prevent diffusion of oxygen, water, and salt to

an underlying metal surface. GO can also potentially strengthen the coating to prevent pit formation that exposes the underlying steel substrate and leads to the formation of rust. In this study, oxygen permeability was found to decrease 7-fold at 1.2 % mass fraction and 4-fold at 2 % mass fraction relative to unfilled WBPU, indicating that GO was an effective barrier for oxygen. On the other hand, water sorption went up at GO loadings greater than 1.2 % mass fraction (e.g. 3.50 % ± 0.11 % for neat WBPU versus 6.90 % ± 0.17 % for 1.2 % mass fraction GO/WBPU at 90 % RH), indicating that GO/WBPU nanocomposites were hygroscopic. Although this is not ideal for a coating meant to prevent corrosion, the corrosion resistance of one specimen of steel coated with GO/WBPU nanocomposite (98 µm ± 7 µm thick,) was still improved by 70 % (-0.036 V for WBPU and -0.056 V for 2 % mass fraction GO/WBPU to reach a large increase in current density (> 0.1 nA) of 1.59 nA and 0.26 nA, respectively) relative to the corrosion resistance of one specimen of steel coated with WBPU (118 µm ± 8 µm thick) as determined by a multiple cyclic potential method in the presence of NaCl (3.5 % mass fraction) over 240 h.[14] Since the performance properties of GO/WBPU nanocomposites were improved relative to unfilled WBPU and the incorporation of GO into WBPU was practical, the durability of these materials was further investigated.

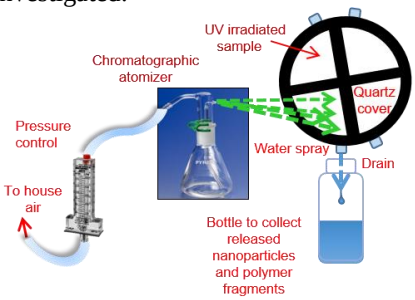

Figure 1: A schematic of the system used for rinsing and collecting run-off water from weathered PNC specimens.

Previously, it was shown that the presence of GO could slow photo-oxidation of WBPU.[9] Furthermore, GO accumulation at the GO/WBPU nanocomposite surface was observed with SEM after UV-weathering. However, GO accumulation was less apparent at longer UV exposure times, indicating that GO might have released from the material surface.[9] Since loss of GO could lead to decreased PNC durability during aging and raise potential EHS issues, methods to measure GO release during UV-weathering were developed.

Two techniques, UV-Vis and Raman spectroscopy were employed in this study since they were previously used to detect GO.[5] Typical uncertainties for these techniques are on the order of 10%, as shown for other CNMs.[15] In UV-Vis spectroscopy, GO absorbs/optically scatters light around 230 nm and red-shifts with decreasing GO flake size and decreasing oxygen functionality.[16-17] Furthermore, the Beer-Lambert law can be used to determine GO mass concentration in aqueous suspension. For Raman spectroscopy, the graphitic nature of GO generates two bands: the G band for the graphitic, sp^2-hybridized network and the D band for the defective, sp^3 sites around the edges, voids, and oxygen functional groups. The D and G bands can be used for detection and sometimes quantification.[10] Both UV-Vis and Raman spectroscopy methods are useful for GO detection and quantification in water. However, PNC run-off suspensions are complex systems that can contain carbonaceous polymer fragments, from which signal intereference can potentially confound the signal from the GO measurement. For this reason, the ability of these methods to detect the total GO concentration in the run-off suspension was first assessed.

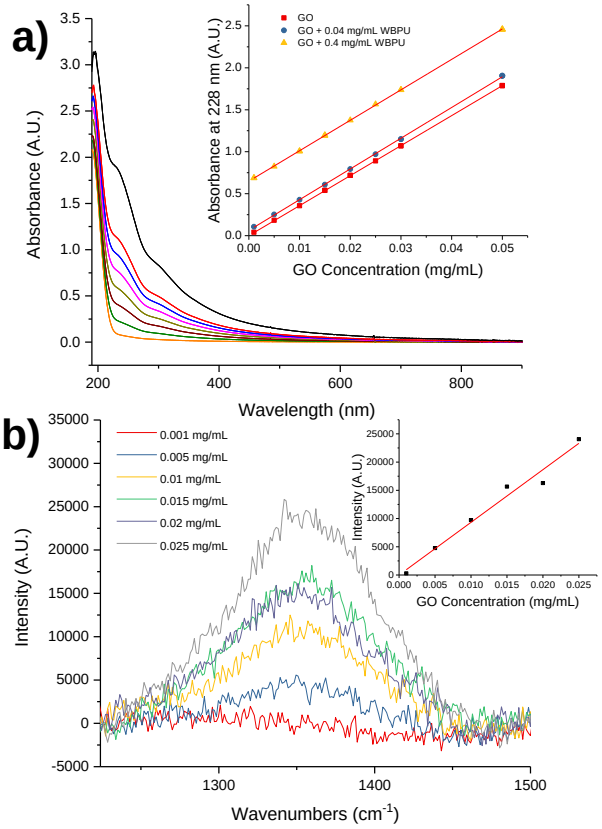

Figure 2: (a) UV-Vis spectra of GO suspensions at different mass concentrations, each containing 0.04 mg/mL WBPU. The inset is the calibration curve of varied GO concentrations with 0, 0.04, and 0.4 mg/mL WBPU. (b) Raman spectroscopy of GO suspensions at different mass concentrations and the associated calibration curve.

In Figure 2a, UV-Vis spectra of different GO mass concentrations in water containing a constant WBPU mass concentration are shown. The inset shows the calibration curves generated from different GO concentrations in the absence of WBPU, with 0.04 mg/mL WBPU, and with 0.4 mg/mL WBPU. The calibration curves shift upwards with added WBPU, indicating that the WBPU affects the absorbance at 230 nm. Furthermore, the 230 nm peak shape becomes obscured at lower GO concentrations when

WBPU is present. This makes detection challenging in the low mg/mL range. This interference is not unique to WBPU as other polymers generally have absorbance bands in the UV range that overlap with the GO band. However, polymers with absorbance bands at longer wavelengths (> 300 nm), can potentially be quantified for concentration in this area of the spectrum to determine the fraction of signal in the UV region originating from GO.

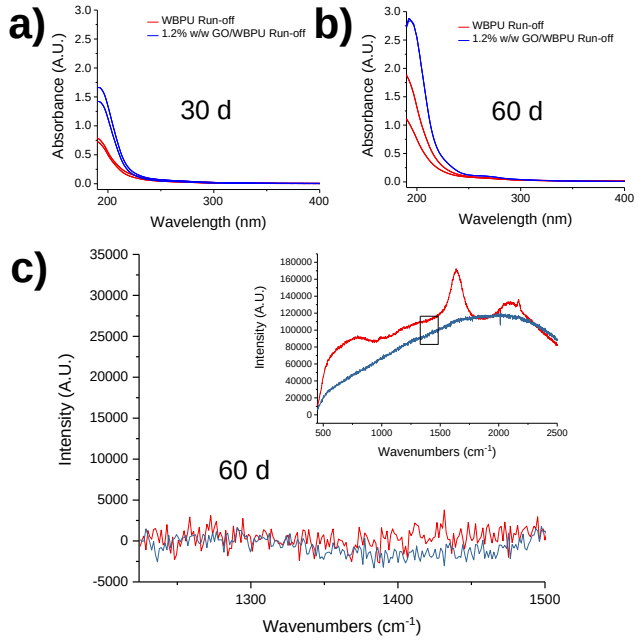

Figure 3: UV-Vis spectra of WBPU (red) and 1.2 % mass fraction GO/WBPU (blue) run-off suspension after (a) 30 d and (b) 60 d (in duplicate) as well as the D band in Raman spectroscopy after 60 d (inset shows full spectrum).

Raman spectroscopy calibration curves were also plotted for the D band of GO in water (Figure 2b). The D band was chosen over the G band as a result of the signal from water deformation that overlapped with the G band.[18] The calibration curve was linear as a function of GO concentration, and there was no signal present in WBPU (not shown). However, the detection limit of GO in water was approximately 5 µg/mL, which was, in part, a result of the background fluorescence associated with GO. Nevertheless, Raman spectroscopy could be used to conclusively determine whether GO was present above 5 µg/mL in this system.

To simulate UV-weathering, 1.2 % mass fraction GO/WBPU and unfilled WBPU were exposed in the NIST SPHERE at 55 °C and 0 % RH. Weathered GO/WBPU nanocomposites and unfilled WBPU were then subjected to simulated rain to remove released materials from the GO/WBPU surfaces (Figure 1). The collected run-off suspensions were analyzed with UV-Vis and Raman spectroscopy (Figure 3). As shown in the UV-Vis spectra, both GO/WBPU and unfilled WBPU run-off suspension contained released material at 30 d (Figure 3a) and 60 d of (Figure 3b) SPHERE exposure. The peak at 230 nm, however, was not apparent for the GO/WBPU run-off suspension. Thus, there was no conclusive indication from UV-Vis spectroscopy that GO had released. However, the amount of material released from the GO/WBPU nanocomposite was much higher than that of the unfilled WBPU as indicated by the approximately doubled absorbance observed in the 200 nm to 300 nm range. Although it is not certain whether GO had released in addition to polymer or whether more polymer had released from the GO/WBPU nanocomposite than unfilled WBPU, it is conclusive that different release characteristics were observed between GO/WBPU and unfilled WBPU.

4 CONCLUSIONS

With the exception of increased water uptake, the mechanical, thermal, and barrier properties of GO/WBPU nanocomposites were improved relative to unfilled WBPU. In terms of GO release, the absence of a distinguishable D band in the Raman spectrum and the absence of a defined UV-Vis absorbance band at 230 nm, indicated that GO detection in the GO/WBPU run-off suspension was not possible. However, UV-Vis indicated that GO/WBPU nanocomposites released more material than unfilled WBPU, either as more polymer or as released GO at or below the 5 µg/mL detection limit of the Raman spectroscopy measurement. Overall, a lack of measurable GO release during accelerated aging combined with enhanced performance properties suggests that GO/WBPU nanocomposites have strong potential for use in commercial applications. Specimens are undergoing further weathering for more detailed analysis.

5 ACKNOWLEDGEMENTS

Goodwin acknowledges the National Research Council for funding to support this project.

REFERENCES

1. Vaia, R. A., et al., *Chem. Mater.* **2007,** *19* (11), 2736-2751.
2. Sung, L., et al., *J. Coat. Technol. Res.* **2015,** *12* (1), 121-135.
3. Kim, H., et al., *Macromol.* **2010,** *43* (16), 6515-6530.
4. Kingston, C., et al., *Carbon* **2014,** *68*, 33-57.
5. Doudrick, K., et al., *Environ. Sci.: Nano* **2015,** *2* (1), 60-67.
6. Harper, S., et al., *J. Phys.: Conf. Ser.* **2015,** *617*, 1-19.
7. Nguyen, T., et al., CRC Press: 2015; pp 315-334.
8. Li, D., et al., *Nat. Nanotechnol.* **2008,** *3* (2), 101-105.
9. Bernard, C., et al., *J. Phys.: Conf. Ser.* **2011,** *304*, 012063/1-012063/8.
10. Celina, M., et al., *Macromol.* **2005,** *38* (7), 2754-2763.
11. Lyon, R. E., et al., *J. ASTM Int.* **2006,** *3* (4), 1-18.
12. Bentz, D., *J. Test. Eval.* **2006,** *35* (3), 1-5.
13. Jacobs, D. S., et al., *J. Coat. Technol. Res.* **2016,** *13* (5), 735-751.
14. Lin, C., et al., *NIST Technical Note 1253,* ***1988****, 19.*
15. NIST, Reference Material 8281, Gaithersburg, MD, 2013.
16. Yousefi, N., et al., *J. Mater. Chem.* **2012,** *22* (25), 12709-12717.
17. Dresselhaus, M. S., et al., *Nano Lett.* **2010,** *10* (3), 751-758.
18. Salzmann, C. G., et al., *Carbon* **2007,** *45* (5), 907-912.